Wing-Store Flutter Analysis of an Airfoil in Incompressible Flow

Zhi-Chun Yang* and Ling-Cheng Zhao†
Northwestern Polytechnic University, Xi'an, China

The flutter of two-dimensional airfoil with external store is analyzed to investigate the effects of pylon stiffness on flutter speed. Among the 40 configurations studied, five were tested in the wind tunnel to verify the analytical results. The variations of wing-store flutter speed with the pylon stiffness can basically be divided into three types. The curves of the normal and flutter frequencies vs pylon stiffness have the same pattern. They can be sketched approximately by the aid of the normal frequencies of the two degenerated two-degree-of-freedom systems, i.e., the freely hinged and rigidly connected store cases. A limiting flutter speed for very small pylon stiffness is deduced, which is useful to identify which type of flutter the configuration studied belongs to.

Nomenclature

ab	= distance of elastic axis A behind the midchord point
b	= wing semichord length
$C(k)$	= $F(k) + iG(k)$ = Theodorsen function
H	= wing plunging displacement, $h = H/b$
$I_\alpha = m_\alpha(r_\alpha b)^2$	= wing moment of inertia about A
$I_\alpha\omega_\alpha^2$	= pitching stiffness of the wing
$I_\beta\omega_\beta^2$	= rotating stiffness of the store relative to the wing
$I_\beta = m_\beta(r_\beta b)^2$	= store moment of inertia about B
$\ell = \bar{\ell}b$	= distance of the hinge point B forward of A
m_h	= plunging mass of the wing system
$m_h\omega_h^2$	= plunging stiffness of the wing
m_α	= pitching mass of the wing
m_β	= mass of the external store
$S_\alpha = m_\alpha x_\alpha b$	= wing mass static moment about A
$S_\beta = m_\beta x_\beta b$	= store mass static moment about B
V	= air speed
α	= wing pitching angle
β	= store rotating angle
ρ	= air density
ω	= vibration frequency, $k = \omega b/V$
$\omega_1,\omega_2,\omega_3$	= 1st, 2nd, and 3rd normal frequency, respectively

Note: All symbols of frequencies and speeds with an overbar, such as $\bar{\omega}_\beta$ and $\bar{V}_F$, represent the corresponding nondimensional frequencies and speeds $\omega_\beta/\omega_\alpha$ and $V_F/b\omega_\alpha$.

Introduction

THE geometrical and physical parameters of the external store have a complicated influence on the wing-flutter characteristics.[1] It is well known that pylon stiffness is a critical parameter. One of the most ingenious devices to suppress wing/store flutter, in which the pylon stiffness plays an important role, is the recently developed decoupler pylon.[2] And for a practical nonlinear flutter analysis, the variation of flutter speed with pylon stiffness must be determined first.[3] The present work deals with a two-dimensional airfoil with external store. Neglecting the aerodynamic forces on the store, the unsteady lift and moment can be predicted fairly well by the Theodorsen formula. For flutter calculation, the V-g method is chiefly used. The p method and time-domain numerical integration have also been used for some intricate cases. Wind-tunnel tests are performed to verify some calculation results.

Wind-Tunnel Test

The two-dimensional wooden wing of a previous study on nonlinear flutter,[4] modified with attachments of two hinged bars as external stores, is used in the present work. The wing-store test setup is shown in the photograph of Fig. 1, along with a brief sketch of the model system. By consideration of the static strength of the model, the test airspeed is limited to lower than 45 m/s. Since the static deflection of the store would be excessively large for very low pylon stiffnesses, no wind-tunnel test has been conducted for such low-stiffness cases.

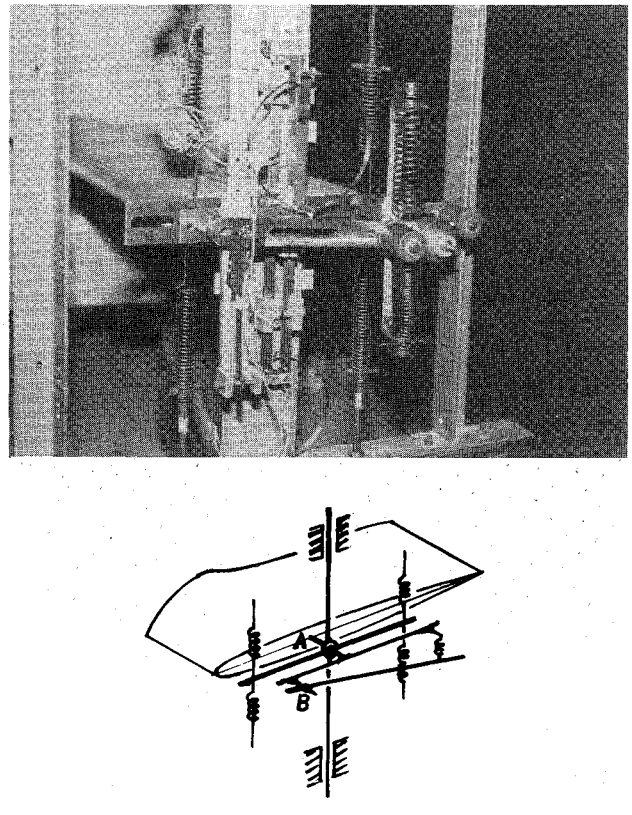

Fig. 1 Wind-tunnel model system.

Received June 7, 1988; revision received Jan. 30, 1989.

*Research Associate, Aircraft Engineering Department.
†Professor, Aircraft Engineering Department.

Mathematical Model

The sketch of a two-dimensional airfoil with external store is shown in Fig. 2. The equation of motion is

$$(m_h + m_\beta)\ddot{H} + (S_\alpha + S_\beta - m_\beta\ell)\ddot{\alpha} + S_\beta\ddot{\beta} + m_h\omega_h^2 H = Q_h \quad (1a)$$

$$(S_\alpha + S_\beta - m_\beta\ell)\ddot{H} + (I_\alpha + I_\beta + m_\beta\ell^2 - 2S_\beta\ell)\ddot{\alpha} + (I_\beta - S_\beta\ell)\ddot{\beta} + I_\alpha\omega_\alpha^2\alpha = Q_\alpha \quad (1b)$$

$$S_\beta\ddot{H} + (I_\beta - S_\beta\ell)\ddot{\alpha} + I_\beta\ddot{\beta} + I_\beta\omega_\beta^2\beta = 0 \quad (1c)$$

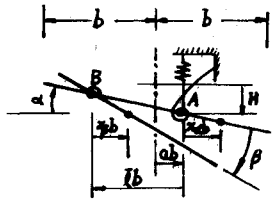

Fig. 2 Mathematical model of wing-store system.

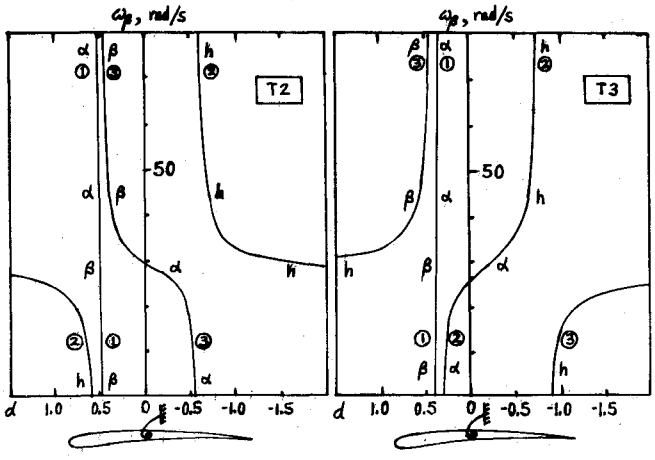

Fig. 3 Node-point position of normal mode.

Since, in the test setup, the mounting of the wing can only translate vertically together with the wing but cannot rotate, the plunging mass m_h and pitching mas m_α are therefore different.

The unsteady air forces Q_h and Q_α are given by

$$Q_h = -\pi\rho b^2(\ddot{H} - ab\ddot{\alpha} + V\dot{\alpha}) - 2\pi\rho bC(k)[\dot{H} + (0.5 - a)b\dot{\alpha} + V\alpha] \quad (2a)$$

$$Q_\alpha = \pi\rho b^2[ab\ddot{H} + (a^2 + 0.125)b^2\ddot{\alpha} - (0.5 - a)bV\dot{\alpha}] + 2\pi\rho Vb^2(0.5 + a)C(k)[\dot{H} + (0.5 - a)b\dot{\alpha} + V\alpha] \quad (2b)$$

Flutter Calculations

In this paper, 40 configurations are analyzed. Six configurations T1–T4, D1, and D2 are relevant to the test models and have the same basic mass parameters, $\mu_h = 133.63$, $\mu_\alpha = 95.96$, $\mu_\beta = 43.36$; except for T4, $\mu_\beta = 21.68$. The remaining 34 configurations are fictitious, with $\mu_h = \mu_\alpha = 12.8$, $\mu_\beta = 4$, $\omega_\alpha = 100$ rad/s, and are composed of three groups, i.e., J, E, and M group, which contain 10, 13, and 11 configurations, respectively. The code name of one configuration, say J60, means that it belongs to the J group with $\omega_h/\omega_\alpha = 60$.

Table 1 Parameters of the configurations analyzed

Code name	a	x_α	r_α^2	$\bar{\ell}$	x_β	r_β^2	b, m
T1, T2, T3, T4	−0.152	0.16	0.44	0.48	0.896	1.015	0.125
D1, D2	−0.152	0.16	0.44	0.48	0.250	0.500	0.125
J-group	−0.410	0.10	0.13	0.18	0.200	0.890	0.118
E-group	−0.410	0.15	0.30	0.18	0.200	0.890	0.118
M-group	−0.340	0.12	0.19	0.20	0.100	0.250	0.118

Table 2 Plunging and pitching frequencies of the test models

	T1	T2	T3	T4	D1	D2
ω_h, rad/s	47.12	47.12	47.12	47.12	47.12	24.00
ω_α, rad/s	59.69	47.00	43.00	43.00	59.69	60.00

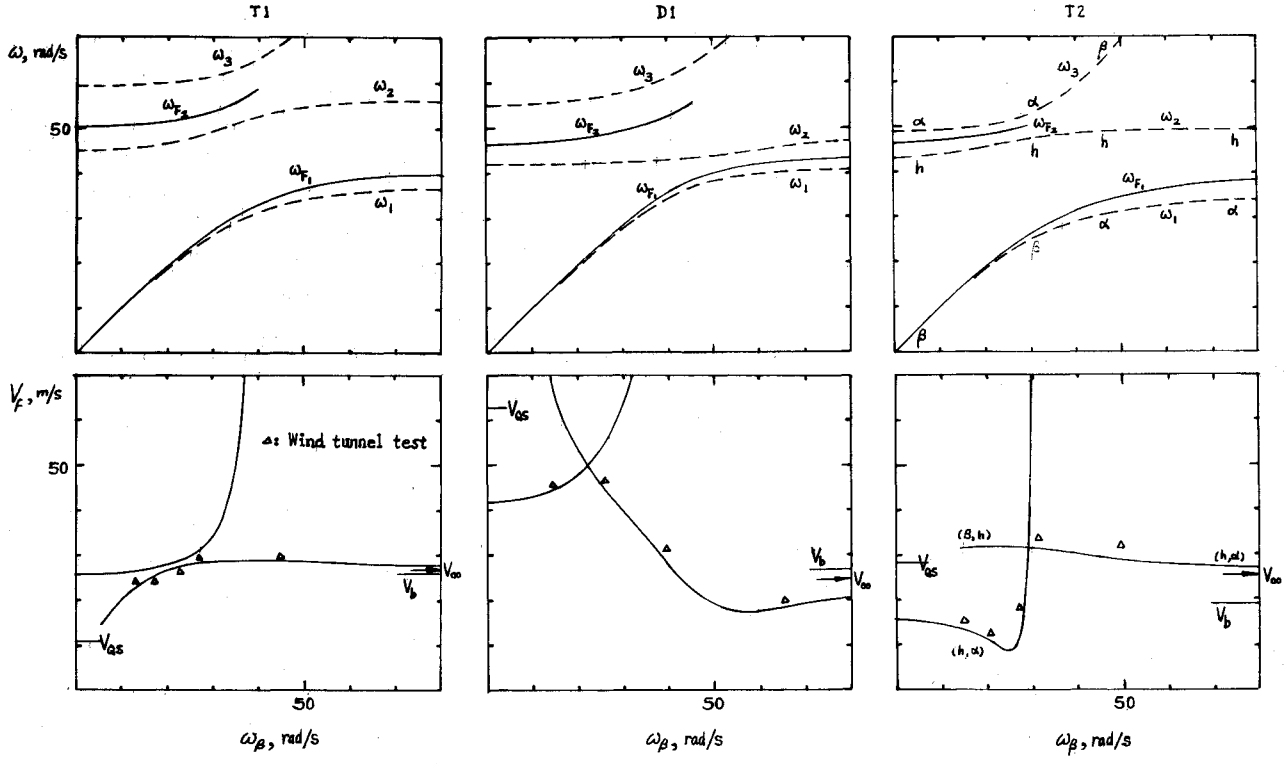

Fig. 4 Natural, flutter frequencies, and flutter speed vs pylon stiffness of T1, D1, and T2.

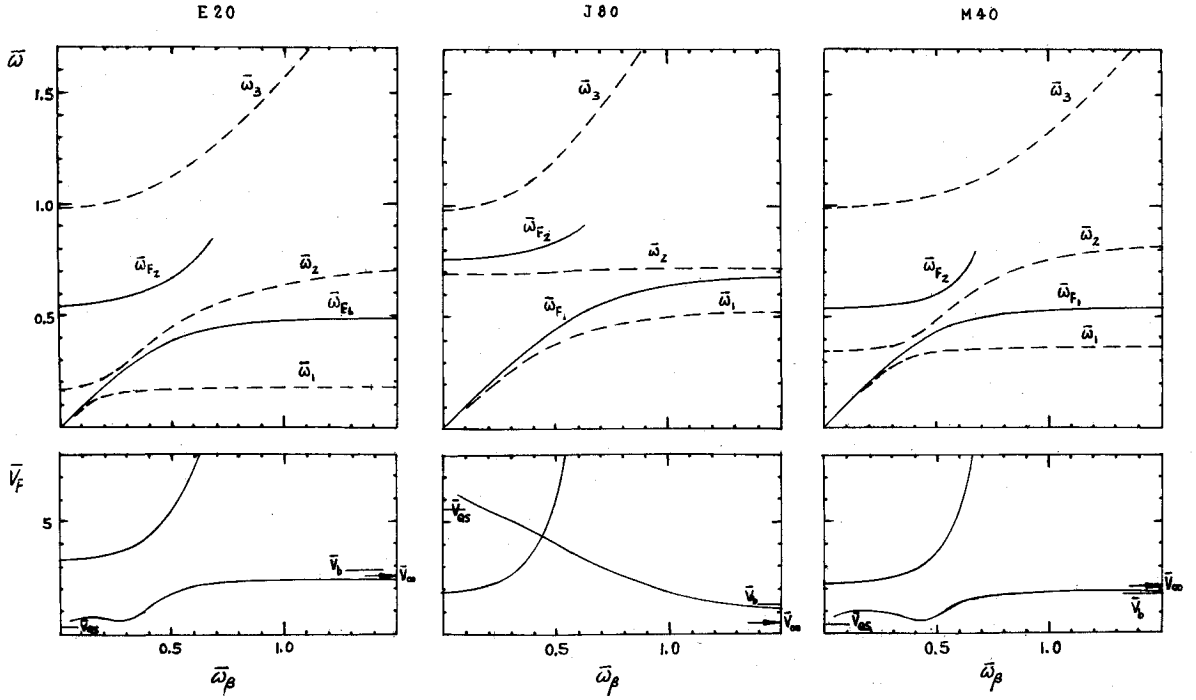

Fig. 5 Natural, flutter frequencies, and flutter speed vs pylon stiff- ness of E20, J80, and M40.

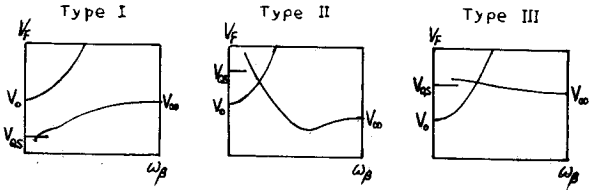

Fig. 6 Three types of flutter boundary.

The other pertinent parameters are listed in Tables 1 and 2. For each configuration with a sequence of selected ω_β, flutter speeds and frequencies are calculated by the V-g method. Let $h = \bar{h}\exp(i\omega t)$, $\alpha = \bar{\alpha}\exp(i\omega t)$, and $\beta = \bar{\beta}\exp(i\omega t)$, then Eqs. (1) and (2) can be reduced to a complex matrix generalized eigenvalue problem, with complex eigenvalue

$$\lambda = (1 + ig)(\omega_\alpha/\omega)^2$$

and eigenvector

$$z = (\bar{h}, \bar{\alpha}, \bar{\beta})^T$$

where g is the structural damping factor and is assumed the same in plunging, pitching, and store rotating in this study.

According to engineering practice of flutter analysis, the eigenvalue problem is transformed first into normal coordinates. The normal modes may be divided into three kinds, i.e., wing-plunging h mode, wing-pitching α-mode, and store-rotating β-mode, or by real-wing terminology, i.e., wing-bending mode, wing-torsion mode, and store-pitching mode. For simplicity, the third one will be called the store mode and be distinguished by the dominant magnitude of the $\bar{\beta}$ element of the eigenvector $[h, \bar{\alpha}, \bar{\beta}]^T$. The remaining two modes are characterized by their $\bar{h}/\bar{\alpha} = d$ value, which indicates the node point position in semichords. The mode with larger d value is the wing-bending mode, whereas the smaller d value denotes the wing-torsion mode. Figure 3 is a plot of the variation of node patterns, which give more visual impression of the change of characters of the modes. It shows also whether the wing motion in a store mode is of the bending or torsion type. In Fig. 3, (i) denotes the ith mode, and the label, such as α, denotes that the mode is a wing-torsion mode. It can be seen that the character of a mode of certain order, say first order, does not keep invariant. For example, the first mode of configuration T2 (see Fig. 3) changes form β-mode to α-mode when ω_β increases form zero to infinity.

Results and Discussion

The results are presented as natural frequency ω_i (i = 1,2,3) and flutter frequency ω_F vs ω_β plots, and flutter speed V_F vs ω_β plot. Six typical plots are shown in Figs. 4 and 5. It can be seen from Fig. 4 that the experimental and calculated results agree well. In the V_F vs ω_β plot, the label (β,α) means that the flutter is of the store pitching-wing torsion mode; V_b and V_∞ denote the flutter speed of the bare wing and the wing with rigidly connected store ($\omega_\beta = \infty$), respectively. V_{QS} is a so-called limiting flutter speed near $\omega_\beta = 0$. It is derived using quasisteady aerodynamics in the Appendix and is found to be useful in the following discussion.

The V_F vs ω_β plot shows that there exist two branches of flutter, one with lower flutter frequency ω_{F1} and another with higher flutter frequency ω_{F2}. In wind-tunnel tests, only the portions of the two branches having the lower flutter speed can be found. These portions comprise a flutter boundary. The patterns of the flutter boundary can be divided into three types, as shown in Fig. 6.

Type I

Only the branch with lower ω_{F1} forms the boundary. Usually, the theoretical value of V_F is quite low in the low ω_β region, but it is the so-called low-damping flutter in which the supercritical condition (i.e., for $V > V_F$) has a g value of very low level, say on the order of 10^{-4}–10^{-6}. Also, the flutter is attributed nearly to only the store mode, and it is somewhat like the natural vibration of the store itself, the wing motion induced could hardly be detected. A small amount of structural damping in the system is sufficient to make this kind of flutter disappear. This means that very low-speed flutter in the case of type I does not exist in reality. When pylon stiffness increases, the flutter may change first to a store-wing bonding (β,h) mode and then to the ordinary wing bending torsion (h, α) mode.

Types II and III

The flutter boundary is formed first by the higher frequency branch in the low ω_β region and then by the lower frequency

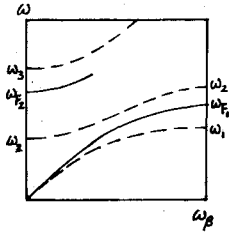

Fig. 7 Variation trends of natural and flutter frequencies vs ω_β.

branch in the high ω_β region. There is a sudden change of the critical mode at the crossing point of the two branches. After the crossing point, for type II, the low-frequency branch drops sharply with increasing ω_β, while for type III, it varies more gently. In general, for type II, V_F at $\omega_\beta = 0$ is higher than V_F at $\omega_\beta = \infty$; this means that the design concept of decoupler pylon is available. On the contrary, the decoupler pylon is ineffective for configurations of type III.

The aforementioned limiting flutter speed V_{QS} together with the flutter speed at $\omega_\beta = 0$ denoted by V_o and the flutter speed at $\omega_\beta = \infty$, i.e., V_∞, can give an estimation of which type of flutter boundary a certain configuration would have.

The estimation is as follows: If $V_{QS} < V_o$, the flutter boundary would be of type I.

If $V_{QS} > V_o$, and $V_o > V_\infty$, it would be of type II.

If $V_{QS} > V_o$, and $V_o < V_\infty$, it would be of type III.

The ω_i and ω_F vs ω_β plots show that for all of the different configurations studied, the curves have a similar pattern as sketched in Fig. 7, which can be roughly determined by the ω_i, ω_F results of the two degenerate two-degree-of-freedom systems for $\omega_\beta = 0$ and $\omega_\beta = \infty$, respectively. In general, when the ω_F and ω_2 curves approach each other very closely, the V_F plot often exhibits a minimum point.

Conclusion

The pylon-stiffness effects on the two-dimensional wing-store system may be depicted by a flutter boundary, which is composed of two branches. The branch with higher flutter frequency has flutter speed rising sharply to infinity with increasing pylon stiffness for the conditions studied, and it would not be of concern in flutter clearance. The branch with lower frequency often gives some critical points for design consideration. The flutter boundary can be divided into three types. A so-called limiting flutter speed near $\omega_\beta = 0$, together with the flutter speeds of the two degenerate two-degree-of-freedom systems both of $\omega_\beta = 0$ and $\omega_\beta = \infty$, can give a sketch of the boundary; hence, a preliminary design judgment of the significance of pylon-stiffness effects can be made before a detailed analysis is performed.

Appendix: Limiting Flutter Speed for Very Low Pylon Stiffness

The governing equation for flutter analysis is

$$[-m_{11}\omega^2 + \mu_{11}\omega_h^2 + 2(F + iG)i\omega V/b]\bar{h} + \{-m_{12}\omega^2 + i\omega V/b + 2(F + iG)[i\omega(0.5 - a)V/b + v^2/b^2]\}\bar{\alpha} - m_{13}\omega^2\bar{\beta} = 0 \tag{A1a}$$

$$[-m_{21}\omega^2 - (1 + 2a)(F + iG)i\omega V/b]\bar{h} + \{-m_{22}\omega^2 + \mu_\alpha r_\alpha^2\omega_\alpha^2 - (1 + 2a)(F + iG)[i\omega V(0.5 - a)/b + V^2/b^2]\} + (0.5 - a)i\omega V/b]\bar{\alpha} - m_{23}\omega^2\bar{\beta} = 0 \tag{A1b}$$

$$-m_{31}\omega^2\bar{h} - m_{32}\omega^2\bar{\alpha} - (m_{33}\omega^2 - m_{33}\omega_\beta^2)\bar{\beta} = 0 \tag{A1c}$$

where

$$\mu_h = m_h/\pi\rho b^2, \qquad \mu_\alpha = m_\alpha/\pi\rho b^2, \qquad \mu_\beta = m_\beta/\pi\rho b^2$$

$$m_{11} = \mu_h + \mu_\beta + 1, \qquad m_{12} = m_{21} = \mu_\alpha x_\alpha + \mu_\beta(x_\beta - \bar{l}) - a$$

$$m_{22} = \mu_\alpha r_\alpha^2 + \mu_\beta(r_\beta^2 + \bar{l}^2 - 2x_\beta\bar{l}) + (a^2 + 0.125)$$

$$m_{13} = m_{31} = \mu_\beta x_\beta, \qquad m_{23} = m_{32} = \mu_\beta(r_\beta^2 - x_\beta\bar{l})$$

$$m_{33} = \mu_\beta r_\beta^2 \tag{A2}$$

The characteristic equations (A1) will be divided into real and imaginary equations, with notations $\Omega = \omega^2$, $\Omega_h = \omega_h^2$, $\Omega_\alpha = \omega_\alpha^2$, and $\Omega_\beta = \omega_\beta^2$. The imaginary equation is

$$(b_1 + b_1')\Omega^2 - (b_1\Omega_\beta + b_2)\Omega + b_2\Omega_\beta = 0 \tag{A3}$$

where

$$b_1 = [2m_{22} + 4am_{12} + m_{11}(2a^2 - 0.5)]F + [m_{11}(0.5 - a) - m_{12}] - [m_{11}(1 + 2a) + 2m_{12} - 2](G/k) \tag{A4a}$$

$$b_1' = \{[-4am_{13}m_{23} + m_{13}^2(0.5 - 2a^2) - 2m_{23}^2]F + m_{13}[m_{23} - m_{13}(0.5 - a)] + [2m_{23} + m_{13}(1 + 2a)]m_{13}(G/k)\}/m_{33} \tag{A4b}$$

$$b_2 = [2\mu_\alpha r_\alpha^2\Omega_\alpha + (2a^2 - 0.5)\mu_h\Omega_h]F + \mu_h\Omega_h(0.5 - a) - \mu_h\Omega_h(1 + 2a)(G/k) \tag{A4c}$$

Equation (A3) may be considered as an algebraic equation of second order. Then for $\Omega_\beta \ll 1$, the root approaching zero can be found as

$$\Omega = b_2\Omega_\beta/(b_2 + b_1\Omega_\beta) + (b_1 + b_1')b_2^2\Omega_\beta^2/(b_2 + b_1\Omega_\beta)^3 + \mathcal{O}(\Omega_\beta^3) \tag{A5}$$

Hence,

$$\Omega_\beta - \Omega = -b_1'\Omega_\beta^2/b_2 \tag{A6a}$$

$$\mu_h\Omega_h(\Omega_\beta - \Omega) = R\Omega_\beta^2 \tag{A6b}$$

where $R = (-b_1'/b_2)\mu_h\Omega_h$.

Since $G/k \to -\infty$ when $\omega \to 0$, $(k \to 0)$, then

$$R = m_{13}[2m_{23} + m_{13}(1 + 2a)]/m_{33}(1 + 2a) \tag{A7}$$

If quasisteady aerodynamic formulas are used with $F = 1$ and $G/k = -2.922$ as suggested,[5] then

$$R = R_1/R_2 \tag{A8a}$$

$$R_1 = [m_{13}m_{23}(4.844 + 4a) + m_{13}^2(2a^2 + 4.844a + 2.922) + 2m_{23}^2]/m_{33} \tag{A8b}$$

$$R_2 = 2\mu_\alpha r_\alpha^2\Omega_\alpha/\mu_h\Omega_h + (2a^2 + 4.844a + 2.922) \tag{A8c}$$

The real equation is

$$a_1\Omega^3 + a_2\Omega^2 + a_3\Omega + a_4 = 0 \tag{A9}$$

where

$$a_1 = (-m_{11}m_{22}m_{33} - 2m_{13}m_{23}m_{12} + m_{11}m_{23}^2 + m_{22}m_{13}^2 + m_{33}m_{12}^2) \tag{A10a}$$

$$a_2 = (m_{11}m_{33} - m_{13}^2)\mu_\alpha r_\alpha^2\Omega_\alpha + (m_{22}m_{33} - m_{23}^2)\mu_h\Omega_h + (m_{11}m_{22} - m_{12}^2)m_{33}\Omega_\beta + F(V/b)^2\,[(1+2a) \times (m_{13}^2 - m_{11}m_{33}) + 2(m_{13}m_{23} - m_{12}m_{33} + m_{33})] + Gk(V/b)^2\,[(0.5 - 2a^2)(m_{11}m_{33} - m_{13}^2) + 4a(m_{13}m_{23} - m_{22}m_{33}) + 2(m_{23}^2 - m_{22}m_{33})] \quad \text{(A10b)}$$

$$a_3 = (-m_{11}m_{33}\mu_\alpha r_\alpha^2\Omega_\alpha - m_{22}m_{33}\mu_h\Omega_h)\Omega_\beta - \mu_h\Omega_h r_\alpha^2\Omega_\alpha m_{33} + F(V/b)^2\,[(1+2a)m_{11}m_{33} + 2(m_{12}m_{33} - m_{33})]\Omega_\beta + F(V/b)^2\,(1+2a)\mu_h\Omega_h m_{33} + Gk(V/b)^2\,[2\mu_\alpha r_\alpha^2\Omega_\alpha - \mu_h\Omega_h(0.5 - 2a^2)]m_{33} + Gk(V/b)^2[m_{11}(2a^2 - 0.5) + 2m_{22} + 4am_{12}]\Omega_\beta \quad \text{(A10c)}$$

$$a_4 = \{\mu_h\Omega_h\, r_\alpha^2\Omega_\alpha^2 - F(V/b)^2\,(1+2a)\mu_h\Omega_h - Gk(V/b)^2\,[2\mu_\alpha r_\alpha^2\Omega_\alpha - \mu_h\Omega_h(0.5 - 2a^2)]\}m_{33}\Omega_\beta \quad \text{(A10d)}$$

For $\Omega_\beta \to 0$, only the root approaching zero is of concern, then F and Gk approach unity and zero, respectively.

Using the expression for $(\Omega_\beta - \Omega)$ given by Eq. (A6a) and neglecting the $\mathcal{O}(\Omega_\beta^3)$ terms, an expression for V can be obtained as

$$V^2 = V_D^2\,[m_{23}^2\mu_h\Omega_h/\mu_\alpha r_\alpha^2\Omega_\alpha + m_{13}^2 - Rm_{33}]/[2m_{13}m_{23}/(1+2a) + m_{13}^2 - Rm_{33}] \quad \text{(A11)}$$

where $V_D = \omega_\alpha b\sqrt{\mu_\alpha r_\alpha^2/(1+2a)}$ is the divergence speed.

If the exact value of R given by Eq. (A7) is used, then Eq. (A11) gives $V = \infty$. This means that $\omega_F \to 0$, $V_F \to \infty$ when $\omega_\beta \to 0$ for any configuration.

This conclusion reveals nothing as to the drastically different flutter features of different configurations for sufficiently small value of ω_β.

If the value of R given by Eq. (A8a) is used, then from Eq. (A11), a more useful value of V can be obtained, which is represented by V_{QS}. From Figs. 4 and 5, it can be seen that V_{QS} can give a fairly good indiction of the flutter feature for ω_β near zero, and it is adequate to call V_{QS} as the limiting flutter speed for very low pylon stiffness. It should be noted that the negative value given by Eq. (A11) is interpreted as an indication of very low flutter speed for ω_β near zero.

References

[1]Mykytow, W. J., et al., "Wing with Store Flutter," AGARD CP-162, April 1975.

[2]Reed, W. H., III, Foughner, J. T., Jr., and Runyan, H. L., Jr., "Decoupler Pylon: A Simple, Effective Wing/Store Flutter Suppressor," *Journal of Aircraft*, Vol. 17, March 1980, pp. 206–211.

[3]Desmarais, R. N. and Reed, W. H., III, "Wing/Store Flutter with Nonlinear Pylon Stiffness," *Journal of Aircraft*, Vol. 18, Nov. 1981, pp. 984–987.

[4]Yang, Z. C. and Zhao, L. C., "Analysis of Limit Cycle Flutter of An Airfoil in Incompressible Flow," *Journal of Sound and Vibration*, Vol. 123, No. 11, May 1988, pp. 1–13.

[5]Goland, M., "The Quasisteady Air Forces for Use in Low-Frequency Stability Calculations," *Journal of the Aeronautical Sciences*, Vol. 17, Oct. 1950, pp. 601–608, 672.